Supporting information for: Revealing the Functional States in the Active Site of BLUF Photoreceptors from Electrochromic Shift Calculations

Florimond Collette, Thomas Renger, and Marcel Schmidt am Busch*

Institut für Theoretische Physik, Johannes Kepler Universität Linz, Altenberger Strasse 69, 4040 Linz, Austria

E-mail: marcel.schmidt_am_busch@jku.at

Phone: +43 732 2468 8549. Fax: +43 732 2468 8540

*To whom correspondence should be addressed

Text S1: Calculation of the Electrochromic Shifts for the Different Mutants S41A, N44A and N45A

Ser41 is present in all 25 coordinates sets. But more than one side-chain conformation is reported. All 10 coordinates sets of 1X0P show a hydrogen bond between Ser41 and the backbone oxygen of Ile37, which orients the side-chain hydroxyl dipole such that the negatively charged oxygen lies in the negative region of highest intensity of the difference potential of the chromophore. On the other side, it places the polar hydrogen closer to the neutral region of the difference potential (Figure 4). The S41A mutation, based on the described Ser41 wild type conformation, should, therefore, lead to a strongly redshifted absorption maximum. We obtain quantitative agreement with the measured value (Table S2) based on the structural information of 1X0P. We conclude that the measured value of 12 nm to the red is consistent with the side-chain conformation proposed in 1X0P.

The 10 coordinates sets of 2HFN show three distinct side-chain conformations of Ser41. The conformations in the coordinates sets B, D and J are as in 1X0P. Again, computed absorption shifts meet the experimental value quantitatively (Table S2). The same side-chain conformation is reported in the two coordinates sets of 2IYG and in coordinates sets A and B of 1YRX. All four computed values agree with the measured 12 nm redshift[S1] (Table S2). The computation of the S41A absorption shift shows that only one out of four proposed side-chain conformations of Ser41 explains the measured wild type-minus-mutant absorption shift. In the remaining three conformations the influence of the polar side-chain hydrogen atom of Ser41 is more pronounced as it moves from the neutral to the more negative region of the difference potential. The distinguished conformation, besides explaining the spectral shift, has the advantage that it is stabilized by a hydrogen bond, which is missing in the remaining three conformations.

Asn44 is not completely conserved among the BLUF proteins (Table S2). In our data set it is present in all coordinates sets of 1X0P and 2HFN, with a reported side-chain conformation

that places the carbonyl oxygen atom away from the isoalloxazine ring system. A hydrogen bond is formed between the C2=O group of the isoalloxazine and the side-chain amide group of Asn44 (Figure 1b). With the exception of this hydrogen atom, the electrostatic influences of the remaining polar side-chain of Asn44 on the absorption maximum of the photoreceptor seem to be balanced. The N44A mutation can therefore be conceived as the elimination of a positive charge from the positive region of intermediate strength of the difference potential, which should yield a redshift, as for S41A, but weaker in magnitude. The quantitative agreement between the computed and measured values for all 20 coordinates sets confirms this hypothesis (Table S2).

Asn45 is a critical residue for the photoreaction and hence it is completely conserved within the BLUF proteins (Figure 3). Its side-chain conformation is similar in the two structural models, $\mathrm{Trp_{in}}$ and $\mathrm{Trp_{out}}$. In all 25 structural templates the side-chain conformation is such that two hydrogen bonds are present between the residue and the flavin chromophore. One hydrogen bond is formed between the the side-chain carbonyl and the N2H group of the chromophore; the second hydrogen bond is between a hydrogen atom of the amide group and the C4=O group of the isoalloxazine. Since the rest of the side-chain is located in regions of weaker difference potential compared to the hydrogen, we assume that the latter is the dominating atom (Figure 4). The N45A mutation should, therefore, result in a blueshifted absorption maximum. Computed absorption shifts meet the experimental value in all cases but we note that absorption shifts based on structures proposing the $\mathrm{Trp_{in}}$ configuration agree somewhat better with the experimental value (Table S2). But we also observe quantitative agreement for 2IYG coordinates set A, which is in the $\mathrm{Trp_{out}}$ configuration. Overall differences are certainly to small to be of any significance for the distinction of $\mathrm{Trp_{in}}$ and $\mathrm{Trp_{out}}$ structural models.

Table S1: Overview of the Different Conformations of the Photoactive Part in the Dark, Transition and Light-Adapted States as Proposed in the Literature ((a) and (b): $Q63_J$ model, (c): $Q63_A$ model); Represented Are the Isoalloxazine Ring System, Tyr21, and Gln63. Domratcheva et al.[S5] and Sadeghian et al.[S6] Propose Identical Dark State Structures

Dark state	Transition state	Light-adapted state
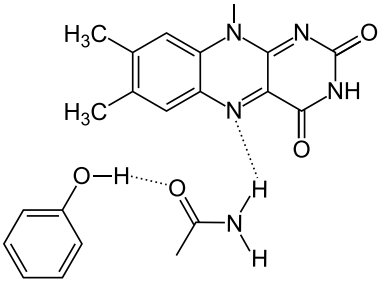 (a) Domratcheva et al.[S5] (b) Sadeghian et al.[S6]	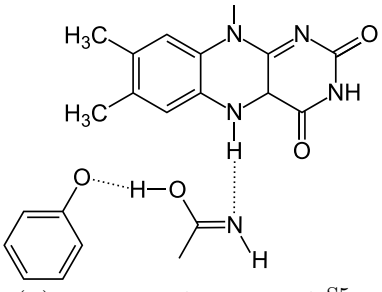 (a) Domratcheva et al.[S5]	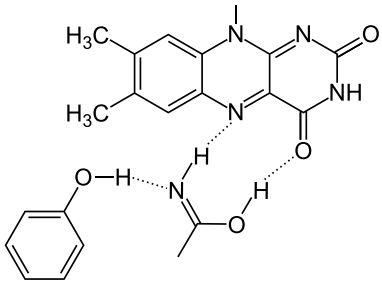 (a) Domratcheva et al.[S5]
	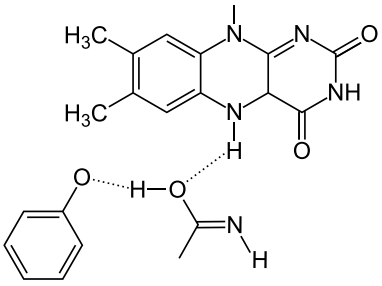 (b) Sadeghian et al.[S6]	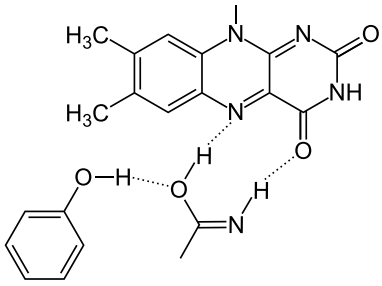 (b) Sadeghian et al.[S6]
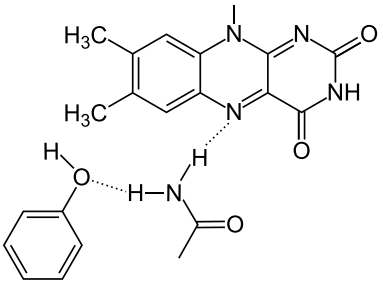 (c) Anderson et al.[S7]		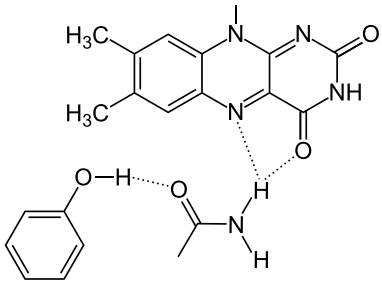 (c) Anderson et al.[S7]

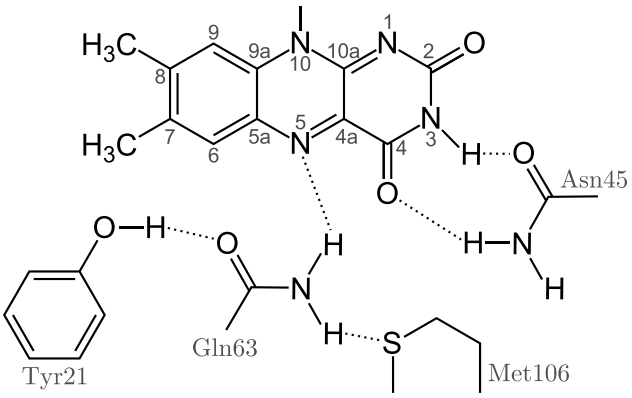

Figure S1: Detailed skeletal structure of the complete photoactive center according to the $Q63_J$ model.[S2–S4]

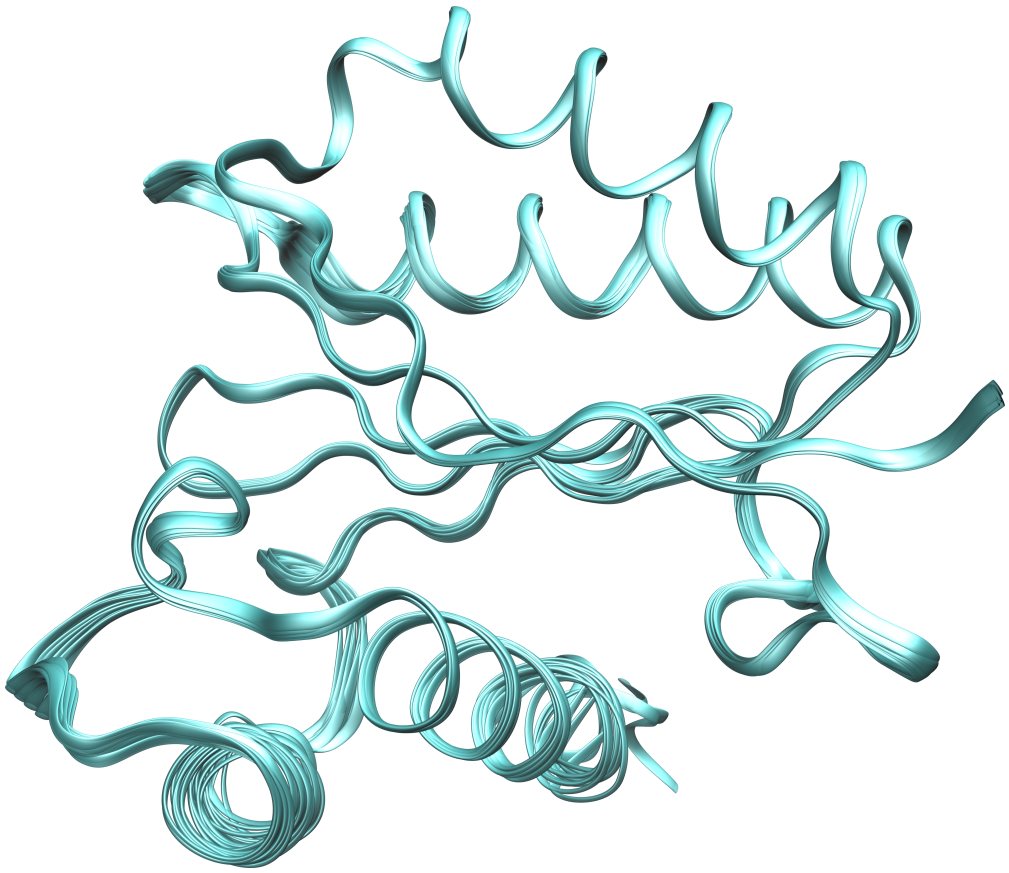

Figure S2: Overlay of the 10 coordinates sets of the 1X0P crystal structure (ribbon diagram).

Table S2: Calculated Absorption Shifts in Units of Nanometer for the Site-Directed Mutants S41A, N44A, N45A, and W104F Using the Structural Data from Different Crystal Structures that Contain Different Coordinates Sets (first column) Which Can Be Assigned to the $Q63_A$ and $Q63_J$ Structural Models (second column); the Experimental Absorption Shifts Are Given in the Last Row (calculated absorption shifts in kilocalorie per mole are given in Table S7)

	type	**S41A**	**N44A**	**N45A**	**W104F**
1YRX A	$Q63_A$	+12.1	*n/a*	−5.3	−1.0
1YRX B	$Q63_A$	+12.5	*n/a*	−5.1	+0.0
1YRX C	$Q63_A$	+6.3	*n/a*	−6.2	−0.6
2HFN D	$Q63_A$	+12.5	+4.1	−5.0	+0.4
1X0P A	$Q63_J$	+13.7	+3.8	−3.8	+0.1
1X0P B	$Q63_J$	+12.9	+4.2	−3.2	+0.1
1X0P C	$Q63_J$	+12.8	+4.0	−3.7	+0.1
1X0P D	$Q63_J$	+12.7	+4.1	−4.3	+0.1
1X0P E	$Q63_J$	+14.2	+4.0	−3.1	+0.1
1X0P F	$Q63_J$	+13.0	+4.5	−2.9	+0.1
1X0P G	$Q63_J$	+14.2	+3.5	−3.5	+0.1
1X0P H	$Q63_J$	+14.0	+4.1	−2.9	+0.1
1X0P I	$Q63_J$	+12.1	+3.6	−3.9	+0.6
1X0P J	$Q63_J$	+14.5	+3.7	−3.9	+0.1
2HFN A	$Q63_J$	+0.6	+4.3	−3.9	+0.1
2HFN B	$Q63_J$	+13.9	+4.4	−3.9	+0.1
2HFN C	$Q63_J$	+0.7	+4.4	−3.5	+0.1
2HFN E	$Q63_J$	−4.6	+4.2	−3.2	+0.1
2HFN F	$Q63_J$	+0.1	+4.1	−3.3	+0.1
2HFN G	$Q63_J$	+1.3	+4.8	−3.8	+0.1
2HFN H	$Q63_J$	−0.2	+4.0	−4.0	+0.1
2HFN I	$Q63_J$	+0.7	+4.2	−3.5	+0.1
2HFN J	$Q63_J$	+12.6	+4.1	−4.1	+0.1
2IYG A	$Q63_J$	+11.6	*n/a*	−4.8	+0.3
2IYG B	$Q63_J$	+11.2	*n/a*	−4.0	+0.3
measured value		+12[a]	+4[b]	−6[b]	−1[a]

[a] See Ref. S1.
[b] See Ref. S2.

Table S3: Calculated Absorption Shifts in Units of Nanometer for the Site-Directed Mutant Q63E Assuming an Anionic State of Glu63 and a Neutral State of Glu63, Where the Proton Makes a Permanent Hydrogen Bond With the C4=O Group of the Chromophore; the Experimental Absorption Shifts Are Given in the Last Row for Comparison

	type	anionic	neutral
1X0P A	$Q63_J$	−54.1	+7.4
1X0P B	$Q63_J$	−50.9	+9.6
1X0P C	$Q63_J$	−57.0	+5.0
1X0P D	$Q63_J$	−53.2	+9.3
1X0P E	$Q63_J$	−52.7	+5.8
1X0P F	$Q63_J$	−50.6	+8.9
1X0P G	$Q63_J$	−49.3	+7.8
1X0P H	$Q63_J$	−50.7	+9.1
1X0P I	$Q63_J$	−54.6	+7.6
1X0P J	$Q63_J$	−53.3	+8.6
2HFN A	$Q63_J$	−55.6	+5.7
2HFN B	$Q63_J$	−53.1	+5.7
2HFN C	$Q63_J$	−53.9	+5.8
2HFN E	$Q63_J$	−54.3	+5.3
2HFN F	$Q63_J$	−54.4	+5.0
2HFN G	$Q63_J$	−57.5	+6.0
2HFN H	$Q63_J$	−54.7	+4.8
2HFN I	$Q63_J$	−54.8	+6.8
2HFN J	$Q63_J$	−52.7	+5.5
2IYG A	$Q63_J$	−56.5	+5.2
2IYG B	$Q63_J$	−59.2	+6.3
measured value		$+3^a$	$+3^a$

[a] See Ref S8.

Table S4: Calculated Absorption Shifts in Units of Nanometer for the Enol Tautomerization of Gln63 Using the Unoptimized Structural Data from Different Coordinates Sets (first column); the Experimental Absorption Shifts Are Given in the Last Row for Comparison

	type	**Q63Q^{enol}**	**Q63Q$^{enol}_{rot}$**
1X0P A	$Q63_J$	+9.7	+12.8
1X0P B	$Q63_J$	+10.4	+13.3
1X0P C	$Q63_J$	+6.9	+10.4
1X0P D	$Q63_J$	+10.7	+13.4
1X0P E	$Q63_J$	+7.2	+10.5
1X0P F	$Q63_J$	+10.0	+12.9
1X0P G	$Q63_J$	+8.9	+12.1
1X0P H	$Q63_J$	+10.4	+13.2
1X0P I	$Q63_J$	+10.2	+12.5
1X0P J	$Q63_J$	+10.2	+12.7
2HFN A	$Q63_J$	+7.4	+9.8
2HFN B	$Q63_J$	+6.8	+9.1
2HFN C	$Q63_J$	+7.3	+9.7
2HFN E	$Q63_J$	+8.2	+10.3
2HFN F	$Q63_J$	+7.2	+9.4
2HFN G	$Q63_J$	+9.3	+11.3
2HFN H	$Q63_J$	+8.1	+10.0
2HFN I	$Q63_J$	+9.0	+10.9
2HFN I	$Q63_J$	+6.2	+8.7
2IYG A	$Q63_J$	+9.0	+10.3
2IYG B	$Q63_J$	+8.2	+10.2
measured value		+10 to +15[a]	+10 to +15[a]

[a] See Ref S2,S9–S12.

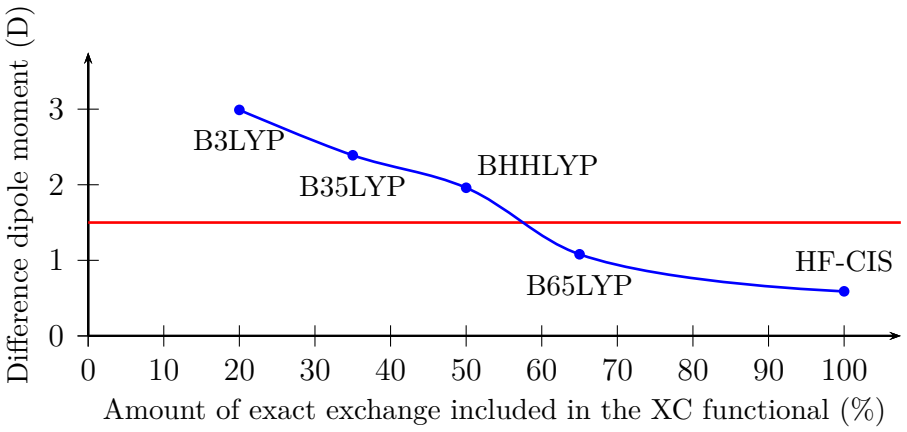

Figure S3: Difference dipole moment of the methyl-isoalloxazine ring system in dependence on the XC functional used in the (TD)DFT calculations[S13] (blue) compared to the experimentally determined value[S14] (red).

Table S5: Computated CHARMM Atomtypes and Atomic Partial Charges (APCs) of the Isoalloxazine Ring System in the Ground and Excited States Obtained with (TD)DFT Using BHHLYP XC Functional.[S13]

atom	type	ground	excited
N1	NF2	−0.680	−0.527
C2	CF3	+0.928	+0.986
O2	ON1	−0.568	−0.549
N3	NF3	−0.800	−0.867
C4	CF3	+0.668	+0.690
O4	ON1	−0.514	−0.534
HF11	HN2	+0.402	+0.414
N5	NF1	−0.632	−0.781
C5A	CF1	+0.689	+0.777
C6	CF2	−0.469	−0.605
HF6	HP	+0.226	+0.231
C7	CF2	+0.238	+0.452
C8	CF2	+0.119	+0.019
C9	CF2	−0.114	−0.107
HF3	HP	+0.136	+0.141
C9A	CF1	−0.465	−0.341
N10	NF1	+0.298	+0.285
C10	CF1	+0.226	+0.304
C4A	CF1	+0.296	−0.018

Table S6: Chosen CHARMM Atomic Partial Charges (APCs) of the Keto-Enol Tautomer of Gln63 Obtained with DFT Using Hartree-Fock XC functional.[S13] All Other Atoms of the Keto-Enol Tautomer Have the Same APCs as for the Standard Glutamine in the Molecular Mechanics Force Field of CHARMM22.

atom	APC
CD	+0.515
OE1	−0.549
HE1	+0.394
NE2	−0.733
HE2	+0.325
CG	+0.132
HG1	+0.090
HG2	+0.090

Table S7: Calculated Absorption Shifts in Units of Kilocalorie per Mole for the Site-Directed Mutants Y21F, Y21I, Y21W, S41A, N44A, N45A, Q63E (neutral, where the proton forms a permanent hydrogen bond to C4=O), Q63L, and W104F and the Enol Tautomerization of Gln63 Using the Structural Data from Different Crystal Structures That Contain Different Coordinates Sets (first column) Which Can Be Assigned to the $Q63_A$ and $Q63_J$ Structural Models (second column); the Experimental Absorption Shifts Are Given in the Last Row

	type	Y21F	Y21I	Y21W	S41A	N44A	N45A	Q63E	Q63E♦	Q63L	Q63Q^{enol}♦	Q63Q$^{enol}_{rot}$♦	W104F
1YRX A	$Q63_A$	−1.74	−1.72	−1.92	−3.69	*n/a*	+1.62	−6.46	*n/a*	−0.91	*n/a*	*n/a*	+0.31
1YRX B	$Q63_A$	−1.57	−1.49	−1.67	−3.81	*n/a*	+1.57	−5.90	*n/a*	−1.08	*n/a*	*n/a*	+0.01
1YRX C	$Q63_A$	−1.47	−1.44	−1.59	−1.92	*n/a*	+1.90	−6.04	*n/a*	−1.81	*n/a*	*n/a*	+0.18
2HFN D	$Q63_A$	−1.69	−1.61	−1.93	−3.83	−1.25	+1.53	−6.55	*n/a*	−1.08	*n/a*	*n/a*	−0.13
1X0P A	$Q63_J$	+1.58	+1.66	+1.44	−4.21	−1.17	+1.16	−1.87	−1.07	+1.21	−3.02	−4.03	−0.03
1X0P B	$Q63_J$	+1.48	+1.57	+1.36	−3.94	−1.28	+0.99	−1.82	−0.95	+0.65	−3.24	−4.37	−0.03
1X0P C	$Q63_J$	+1.50	+1.59	+1.36	−3.93	−1.23	+1.12	−1.66	−0.89	+2.10	−2.09	−3.25	−0.03
1X0P D	$Q63_J$	+1.50	+1.59	+1.37	−3.90	−1.26	+1.31	−1.88	−1.10	+0.76	−3.43	−4.34	−0.03
1X0P E	$Q63_J$	+1.41	+1.48	+1.31	−4.35	−1.22	+0.93	−1.55	−0.93	+1.55	−2.39	−3.31	−0.03
1X0P F	$Q63_J$	+1.45	+1.56	+1.31	−3.97	−1.37	+0.89	−1.77	−1.07	+0.81	−3.27	−4.15	−0.03
1X0P G	$Q63_J$	+1.48	+1.56	+1.35	−4.35	−1.06	+1.07	−1.65	−0.76	+0.96	−2.84	−3.97	−0.03
1X0P H	$Q63_J$	+1.58	+1.68	+1.43	−4.28	−1.26	+0.90	−1.75	−1.03	+0.48	−3.43	−4.27	−0.03
1X0P I	$Q63_J$	+1.44	+1.54	+1.33	−3.70	−1.11	+1.21	−1.82	−1.40	+1.01	−3.30	−3.90	−0.18
1X0P J	$Q63_J$	+1.56	+1.65	+1.45	−4.44	−1.13	+1.20	−1.78	−1.30	+0.86	−3.36	−4.03	−0.03
2HFN A	$Q63_J$	+1.45	+1.52	+1.23	−0.18	−1.32	+1.20	−1.62	−1.32	+1.86	−2.58	−2.99	−0.02
2HFN B	$Q63_J$	+1.43	+1.50	+1.23	−4.26	−1.35	+1.19	−1.46	−1.05	+1.64	−2.67	−2.77	−0.03
2HFN C	$Q63_J$	+1.38	+1.43	+1.29	−0.21	−1.34	+1.06	−1.56	−1.39	+1.79	−2.46	−3.00	−0.03
2HFN E	$Q63_J$	+1.43	+1.49	+1.19	+1.42	−1.28	+0.97	−1.60	−1.68	+1.77	−2.24	−3.15	−0.03
2HFN F	$Q63_J$	+1.42	+1.49	+1.21	−0.02	−1.27	+1.00	−1.49	−1.26	+1.81	−2.41	−2.86	−0.02
2HFN G	$Q63_J$	+1.49	+1.58	+1.27	−0.39	−1.47	+1.17	−1.82	−1.48	+1.75	−3.11	−3.45	−0.03
2HFN H	$Q63_J$	+1.42	+1.52	+1.22	+0.07	−1.22	+1.23	−1.57	−1.34	+1.72	−2.63	−3.03	−0.03
2HFN I	$Q63_J$	+1.40	+1.49	+1.31	−0.23	−1.28	+1.08	−1.71	−1.37	+1.44	−3.22	−3.36	−0.03
2HFN J	$Q63_J$	+1.32	+1.38	+1.11	−3.85	−1.27	+1.27	−1.37	−1.19	+1.93	−2.10	−2.65	−0.04
2IYG A	$Q63_J$	+1.84	+1.90	+1.58	−3.56	*n/a*	+1.48	−1.59	−0.87	+1.80	−2.87	−3.07	+0.00
2IYG B	$Q63_J$	+1.62	+1.64	+1.42	−3.44	*n/a*	+1.22	−1.72	−0.62	+2.34	−2.94	−2.97	+0.00

♦ The side-chain orientation of Gln63 has been manipulated in order to simulate the hydrogen bond distance between the side-chain amide and the C4=O of the isoalloxazine as related for the light-adapted state according to spectroscopic data (see text).

References

(S1) Bonetti, C.; Stierl, M.; Mathes, T.; van Stokkum, I. H. M.; Mullen, K. M.; Cohen-Stuart, T. A.; van Grondelle, R.; Hegemann, P.; Kennis, J. T. M. The Role of Key Amino Acids in the Photoactivation Pathway of the *Synechocystis* Slr1694 BLUF Domain. *Biochemistry* **2009**, *48*, 11458–11469.

(S2) Kita, A.; Okajima, K.; Morimoto, Y.; Ikeuchi, M.; Miki, K. Structure of a Cyanobacterial BLUF Protein, Tll0078, Containing a Novel FAD-Binding Blue Light Sensor Domain. *J. Mol. Biol.* **2005**, *349*, 1–9.

(S3) Jung, A.; Domratcheva, T.; Tarutina, M.; Wu, Q.; Ko, W.-h.; Shoeman, R. L.; Gomelsky, M.; Gardner, K. H.; Schlichting, I. Structure of a Bacterial BLUF Photoreceptor: Insights into Blue Light-Mediated Signal Transduction. *Proc. Natl. Acad. Sci. U.S.A.* **2005**, *102*, 12350–12355.

(S4) Jung, A.; Reinstein, J.; Domratcheva, T.; Shoeman, R. L.; Schlichting, I. Crystal Structures of the AppA BLUF Domain Photoreceptor Provide Insights into Blue Light-Mediated Signal Transduction. *J. Mol. Biol.* **2006**, *362*, 717–732.

(S5) Domratcheva, T.; Grigorenko, B. L.; Schlichting, I.; Nemukhin, A. V. Molecular Models Predict Light-Induced Glutamine Tautomerization in BLUF Photoreceptors. *Biophys. J.* **2008**, *94*, 3872–3879.

(S6) Sadeghian, K.; Bocola, M.; Schütz, M. A Conclusive Mechanism of the Photoinduced Reaction Cascade in Blue Light Using Flavin Photoreceptors. *J. Am. Chem. Soc.* **2008**, *130*, 12501–12513.

(S7) Anderson, S.; Dragnea, V.; Masuda, S.; Ybe, J.; Moffat, K.; Bauer, C. Structure of a Novel Photoreceptor, the BLUF Domain of AppA from *Rhodobacter sphaeroides*. *Biochemistry* **2005**, *44*, 7998–8005.

(S8) Lukacs, A.; Haigney, A.; Brust, R.; Zhao, R.-K.; Stelling, A. L.; Clark, I. P.; Towrie, M.; Greetham, G. M.; Meech, S. R.; Tonge, P. J. Photoexcitation of the Blue Light Using FAD Photoreceptor AppA Results in Ultrafast Changes to the Protein Matrix. *J. Am. Chem. Soc.* **2011**, *133*, 16893–16900.

(S9) Gomelsky, M.; Kaplan, S. AppA, a Redox Regulator of Photosystem Formation in *Rhodobacter sphaeroides* 2.4.1, Is a Flavoprotein. *J. Biol. Chem.* **1998**, *273*, 35319–35325.

(S10) Masuda, S.; Bauer, C. E. AppA Is a Blue Light Photoreceptor That Antirepresses Photosynthesis Gene Expression in *Rhodobacter sphaeroides*. *Cell* **2002**, *110*, 613–623.

(S11) Iseki, M.; Matsunaga, S.; Murakami, A.; Ohno, K.; Shiga, K.; Yoshida, K.; Sugai, M.; Takahashi, T.; Hori, T.; Watanabe, M. A Blue-Light-Activated Adenylyl Cyclase Mediates Photoavoidance in *Euglena gracilis*. *Nature* **2002**, *415*, 1047–1051.

(S12) Masuda, S.; Hasegawa, K.; Ishii, A.; Ono, T.-A. Light-Induced Structural Changes in a Putative Blue-Light Receptor with a Novel FAD Binding Fold Sensor of Blue-Light Using FAD (BLUF); Slr1694 of *Synechocystis* sp. PCC6803. *Biochemistry* **2004**, *43*, 5304–5313.

(S13) Madjet, M. E.-A.; Abdurahman, A.; Renger, T. Intermolecular Coulomb Couplings from Ab Initio Electrostatic Potentials: Application to Optical Transitions of Strongly Coupled Pigments in Photosynthetic Antennae and Reaction Centers. *J. Phys. Chem. B* **2006**, *110*, 17268–17281.

(S14) Stanley, R. J.; Siddiqui, M. S. A Stark Spectroscopic Study of $N(3)$-Methyl, $N(10)$-Isobutyl-7,8-Dimethylisoalloxazine in Nonpolar Low-Temperature Glasses: Experiment and Comparison with Calculations. *J. Phys. Chem. A* **2001**, *105*, 11001–11008.